Electrospray Deposition of C_{60} on a Hydrogen-Bonded Supramolecular Network

Alex Saywell,[†] Graziano Magnano,[†] Christopher J. Satterley,[†] Luís M. A. Perdigão,[†] Neil R. Champness,[‡] Peter H. Beton,[†] and James N. O'Shea*[,†]

Schools of Physics & Astronomy and Chemistry, University of Nottingham, Nottingham NG7 2RD, U.K.

Received: December 21, 2007; Revised Manuscript Received: March 3, 2008

An electrospray technique has been successfully used to deposit C_{60} onto a hydrogen-bonded supramolecular template held in an ultrahigh vacuum environment. Characterization of the surface by *in situ* scanning tunneling microscopy shows the size-selective trapping of C_{60} dimers and heptamers within a 3,4,9,10-perylene tetracarboxylic diimide (PTCDI)/melamine network. We demonstrate that ultrahigh vacuum electrospray deposition (UHV-ESD), where energetic molecules impact onto a substrate, is compatible with surfaces which have been functionalized through the incorporation of hydrogen-bonded templates.

Introduction

Within the rapidly developing area of nanoscience, there is great interest in systems which combine ordered nanoscale structures with novel optical, electronic, and magnetic properties.[1–5] The ability to produce nanoscale structured materials with predetermined geometries is of paramount importance to the future production of nanodevices. Unfortunately, many of the molecules with potential for the manufacture of nanomaterials (e.g., functionalized/endohedral fullerenes, porphyrins, single molecule magnets) are thermally labile and as such may not be deposited in vacuum by conventional methods such as sublimation. Electrospray (ES) ionization provides a highly promising route for the deposition of nonvolatile molecules onto surfaces in ultrahigh vacuum (UHV). The technique is widely used in mass spectroscopy to introduce large and fragile molecules into the gas phase,[6] and it has shown promise as a method of depositing polymers and biomolecules[7,8] into vacuum. We have previously demonstrated that carbon nanotubes can be deposited from a liquid suspension onto a surface held in high vacuum using an *in vacuo* implementation of ES ionization with *ex situ* characterization using atomic force microscopy.[9] More recently, we have shown that differential pumping of an ES molecular beam from air to UHV can be used to deposit fullerene molecules from solution onto a Au(111) surface at pressures as low as 1×10^{-8} mbar for *in situ* scanning tunneling microscopy (STM) and synchrotron-based electron spectroscopy studies.[10]

Although the UHV-ESD of molecules (C_{60}) onto metal substrates has been demonstrated,[10] little is known about how the ES deposition (ESD) process could affect surfaces that have been functionalized by supramolecular networks. The formation of two-dimensional supramolecular structures has been extensively studied,[11–27] and it has been shown that such structures may be used to facilitate the production of well-ordered templates with network cavities with dimensions on the order of nanometers. Such nanoscale templates are ideally suited to the capture of additional moieties which may be used to further functionalize the surface. A number of studies on the host–guest architecture of molecular species, deposited by conventional thermal methods, trapped within the pores of supramolecular structures have been carried out,[12–21] but until now the compatibility between the use of ES deposition and self-assembled templates has not been explored.

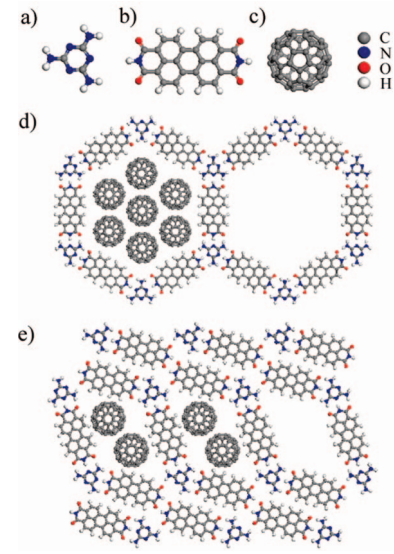

Figure 1. (a−c) Chemical structures of melamine, PTCDI, and C_{60}. Panels (d) and (e) show the previously proposed structures for two hydrogen-bonded supramolecular networks which may be formed on the Au(111) surface, with hexagonal and parallelogram geometries. Earlier work has shown that the open pores of these networks may trap either heptamers or dimers of C_{60}, depending upon the dimensions of the network cavities. The diagrams here show possible orientations for the trapped molecules.

We address the question of the potentially destructive nature of UHV-ESD by studying a previously investigated bimolecular network, formed from 1,3,5-triazine-2,4,6-triamine (melamine) and 3,4,9,10-perylene tetracarboxylic diimide (PTCDI) (molecular structures shown in Figure 1a and b), as a test system for the UHV-ESD of C_{60}. These molecular "building blocks" are known to self-assemble into open-pored hexagonal[18] and parallelogram[19] networks when codeposited upon a Au(111) substrate and subjected to the appropriate annealing conditions (the proposed structures for the hexagonal and parallelogram networks are shown in Figure 1d and e, respectively). Deposition of fullerenes, from a Knudsen cell in UHV, onto the network results in the size-selective trapping of heptamers and dimers

* To whom correspondence should be addressed. Telephone: +44 (0) 115 9515149. Fax: +44 (0) 115 9515180. E-mail: james.oshea@nottingham.ac.uk.
† School of Physics & Astronomy.
‡ School of Chemistry.

10.1021/jp7119944 CCC: $40.75
Published on Web 04/30/2008

in the hexagonal and parallelogram network pores, respectively. These previous studies provide the ideal experimental background to analyze the effects of substituting a thermal deposition technique for UHV-ESD. Here, we report a methodology for the UHV-ESD of molecular species onto hydrogen-bonded networks and provide evidence that the test system of ES C_{60} deposited upon a bimolecular melamine/PTCDI network produces structures that are comparable to those produced by thermal deposition.

Experimental Methods

A 4 mm × 8 mm gold on mica substrate (thickness of 1500 Å; supplied commercially by Agilent) was loaded into a UHV system with a base pressure of 5×10^{-11} Torr. The sample was cleaned by Ar ion sputtering (6×10^{-6} Torr, 1 keV, ~3 μA) and subsequent annealing (~500 °C). Images of the surface were acquired using a scanning tunnelling microscope, housed within the UHV system, using electrochemically etched tungsten tips, and operating in constant current mode at room temperature.[28] Images of the surface taken after the sputter−anneal cycle show the characteristic ($22 \times \sqrt{3}$) herringbone reconstruction of the Au(111) surface.[29] The supramolecular network was prepared by the sequential deposition of PTCDI and melamine, using Knudsen cells, followed by a short anneal at ~100 °C as described previously.[19] This process facilitates the formation of two coexisting bimolecular networks: one with hexagonal pores and the other with parallelogram shaped pores (the structures of these networks are shown in Figure 1d and e, respectively).

Using UHV-ESD, C_{60} was transferred onto the network from a solution of toluene/acetonitrile (1 mg/mL of C_{60} dissolved in a 4:1 solution, by volume). The ES experimental apparatus, built in-house, has already been described in detail elsewhere.[10] In summary, a solution containing the molecules to be deposited is passed through a stainless steel emitter held at ~2 kV at a typical flow rate of 10 μL/min. This leads to the formation of a spray at atmospheric pressure outside the UHV system. The spray enters the UHV system via an aperture, passes through a series of differentially pumped chambers, and impinges upon the sample situated within a preparation chamber having a base pressure of 5×10^{-11} Torr. The pressure in the sample preparation chamber while open to the differential pumping system, but in the absence of spray, is $\sim 10^{-9}$ Torr. During ES deposition, the pressure rises to $\sim 10^{-7}$ Torr, with the additional pressure being due solely to the presence of the solvent molecules within the preparation chamber (ascertained by residual gas analysis).

Results and Discussion

Supramolecular hydrogen-bonded structures were formed on a Au(111) substrate, as described above, giving rise to coexisting bimolecular networks with hexagonal[18] and parallelogram[19] shaped pores. Figure 2 shows STM images of the network produced prior to the ES deposition of C_{60}. Figure 2a is an STM topograph showing several small domains of the parallelogram network (labeled A). Regions of the parallelogram network with dimensions of 20 nm × 20 nm were typically observed. Islands of close-packed PTCDI[30] (labeled B) which have not been converted into the network arrangement are seen to coexist with the hydrogen-bonded networks as well as with regions of the gold substrate (labeled C). Although the majority of the ordered structures are composed of the parallelogram network, under these annealing conditions, small regions of the hexagonal network are also observed (shown in Figure 2c).

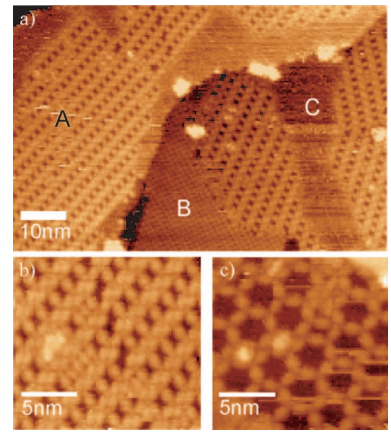

Figure 2. (a) STM image showing the types of structures formed upon the Au(111) surface after the creation of a parallelogram network ($V_{sample} = -2.00$ V, $I_{tunnel} = 0.03$ nA, 85.9 nm × 56.7 nm). Area A shows a large domain of the parallelogram network, while B is a region of close-packed PTCDI. Region C is an area of gold which is free from adsorbed molecules. (b) Higher resolution image showing the internal structure of the parallelogram network ($V_{sample} = -1.80$ V, $I_{tunnel} = 0.03$ nA, 17.0 nm × 14.0 nm). (c) STM image of the internal structure of the hexagonal network which exists alongside the parallelogram network ($V_{sample} = -1.80$ V, $I_{tunnel} = 0.03$ nA, 15.1 nm × 12.4 nm).

The series of STM images shown in Figure 3 provide insight into the effect of energetic C_{60} and solvent molecules colliding with the network structure during ES deposition. Figure 3a shows an image of the surface morphology after a 2 min ES deposition of C_{60}. From the image, it is possible to identify several areas of interest. The dashed box labeled A shows a region of a parallelogram network with rows of C_{60} dimers trapped within the pores. Area B is a region of a hexagonal network with C_{60} heptamers filling the pores, while part C shows an area of a network which appears to have been reordered during ES deposition. The area to the right of the image is a large island of close-packed PTCDI and is free of adsorbed C_{60}. Figure 3b shows an area with a similar structure as that of region B, where a regular array of trapped C_{60} clusters, with each cluster being formed from seven molecules in a hexagonal arrangement, are identified as heptamers trapped in the hexagonal shaped pores of the underlying network structure. Second layer growth of C_{60} is also observed, with the extra layer of molecules filling the spaces in between the trapped heptamers, leading to the "bright" open pored structure seen in the center of the image. The images shown here compare well with results obtained following sublimation of C_{60} onto a hexagonal network,[12] producing structures analogous to those seen in Figure 3b. The "streaky" scan lines observed in the top section of the image are indicative of the presence of diffusive molecules, suggesting that some molecules are not completely immobilized by the presence of the network. Trapped C_{60} dimers mixed in among the heptameric structure demonstrate that defects, of the type reported in previous work,[18] are also present on the surface.

Due to their size and shape, the parallelogram network pores provide trap sites for dimers of C_{60}.[19] The bright rectangular features present in the central region of the images shown in Figure 3a (region A) and c have a periodicity, and an apparent height, which agrees with that previously measured for the thermally deposited C_{60} trapped within the parallelogram network pores (dimensions of 30.7 ± 0.4 Å by 19.4 ± 0.3 Å (ref 19) and an apparent height of ~6 Å), allowing us to attribute these features to trapped C_{60} dimers. The observed size-selective trapping of the C_{60} dimers within the pores of the parallelogram network is in excellent agreement with previous thermal

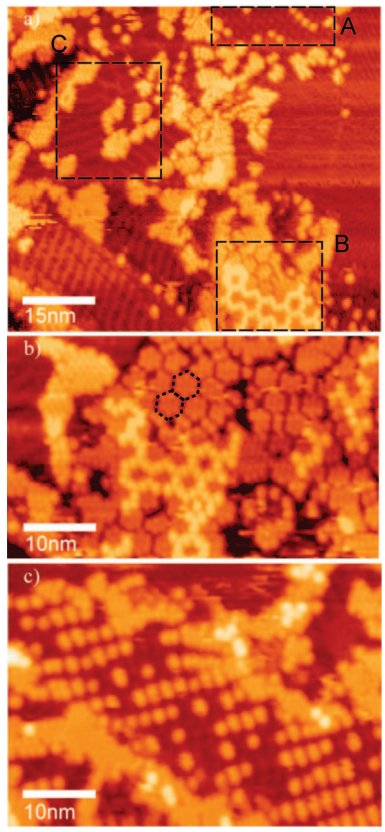

Figure 3. STM images of the surface after electrospray deposition of C_{60}. (a) The surface after being subjected to 2 min of electrospray deposition of C_{60} from a solution of toluene/acetonitrile (1 mg/mL of C_{60} dissolved in a 4:1 solution, by volume). The areas marked A−C demonstrate the three different surface morphologies observed (V_{sample} = +1.80 V, I_{tunnel} = 0.03 nA, 102.3 nm × 75.3 nm). (b) Area of hexagonal network pores filled with heptamers of C_{60} (similar morphology to that of area B highlighted in (a)). The two hexagonal cells highlighted are two heptameric clusters of C_{60} trapped within the network pores. In the bottom part of the image, a second layer of C_{60} growth is observed, forming a bright, open pored, hexagonal array (V_{sample} = +1.80 V, I_{tunnel} = 0.03 nA, 51.6 nm × 31.0 nm). (c) Region of a parallelogram network which has trapped several C_{60} dimers (similar morphology to that of area A highlighted in (a)). (V_{sample} = +1.80 V, I_{tunnel} = 0.03 nA, 51.6 nm × 36.4 nm).

deposition experiments.[19] In addition to the trapped molecules, there are several islands of close-packed C_{60} visible in the image. These islands have the same apparent height as the dimers, indicating that the close-packed domains are formed on the clean Au(111) surface and not on top of the PTCDI regions. Areas of close-packed PTCDI (e.g., the region to the right of the image in Figure 3a) are free from C_{60}, providing further evidence that the adsorption of C_{60} onto PTCDI is unfavorable, as observed in the previous sublimation experiments. The similarities between the arrangements of the trapped dimers, and the preferential formation of C_{60} islands upon areas of clean gold, produced by the two different deposition techniques leads us to postulate that the surface mobility of C_{60} is not changed significantly by altering the method of deposition.

Some areas of the supramolecular network have undergone a reordering process during the ES deposition procedure. Figure 4a and b shows STM images of surface domains that have different morphologies from those observed prior to ES deposition. Figure 4a shows a "mixed" phase of PTCDI and melamine where rows of PTCDI are stacked side by side and are separated by rows of close-packed melamine. This structure has been observed previously, and it is produced after the codeposition

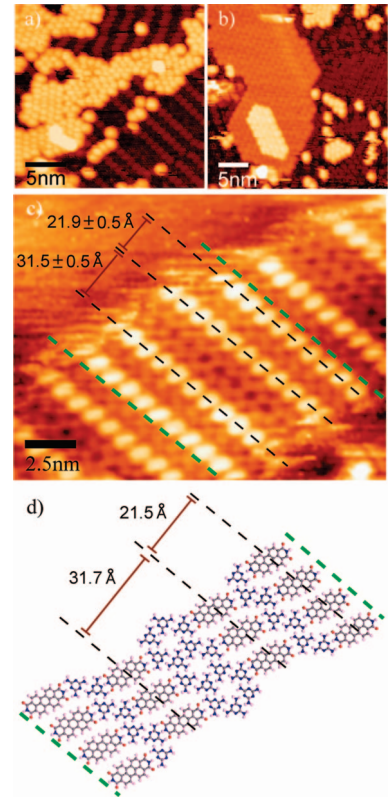

Figure 4. (a) Area of network that has been reordered. The regular hydrogen bonding structure of the network has been altered, leading to a "mixed" phase of melamine and PTCDI (V_{sample} = +1.80 V, I_{tunnel} = 0.03 nA, 23.9 nm × 23.9 nm). (b) Multiple layers of close-packed PTCDI have been produced as a byproduct of the network reorganization (V_{sample} = +1.80 V, I_{tunnel} = 0.03 nA, 32.9 nm × 33.9 nm). (c) High resolution image of the "mixed" phase structure showing rows of PTCDI separated by regions of melamine; the experimentally determined dimensions are shown (image is taken from a different set of experiments). (d) Model of the "mixed" phase of PTCDI and melamine with dimensions calculated using hydrogen bond distances obtained from DFT calculations.

of melamine and PTCDI, prior to the further annealing stage which is required to form the network. It is similar to, but more ordered than, one of the mixed phases identified in ref 18. Figure 4c is a high resolution image (taken from a different set of experiments during the annealing stages of the formation of the supramolecular network) showing the internal structure of the "mixed" phase. A proposed structure for this phase is presented in Figure 4d; the structural dimensions were determined using the theoretical hydrogen bond distances for the PTCDI/melamine and melamine/melamine pairs calculated from density functional theory (DFT).[31] The experimentally measured distances are found to be in good agreement with the values estimated from calculations (shown in Figure 4d). As this "mixed" structure is not present on the surface before ES deposition (and is not observed as an effect of thermal sublimation), we conclude that the network reordering is associated with the ES deposition process.

The melamine/PTCDI ratio for this "mixed" structure is approximately 2:1 and is greater than the equivalent ratio for the hexagonal and parallelogram networks, with both being 2:3. Therefore, if a reordering process were to occur during the ES process, areas with an excess of PTCDI would be expected on the surface. The result of this reordering is shown in Figure 4b where, by analyzing the apparent height of the PTCDI islands, it can be seen that three distinct layers of close-packed PTCDI

have been formed. All PTCDI islands before UHV-ESD were only one molecule high; therefore, the resulting multilayered structure of islands following deposition provides evidence for the removal of PTCDI molecules from the bimolecular network during the creation of the "mixed" phase.

Image analysis of the STM data allows a quantitative picture to be obtained of the differences between the surface coverage of the supramolecular structures before and after the UHV-ESD of C_{60}. The overall melamine to PTCDI ratio, 1:2, is unaffected by exposure to electrospray deposition, but the relative abundance of the various phases does change. The coverage of the parallelogram network is reduced from 48 ± 9% before UHV-ESD to 15 ± 8% afterward. Conversely, the coverages of both the "close-packed" (PTCDI only) and "mixed" (melamine rich) molecular arrangements increase from ~10% to ~20% and from 0% to ~20%, respectively, suggesting the conversion of the parallelogram network into other phases.

It is possible that network reordering is mediated by solvent droplets arriving at the surface. Subsequent evaporation of the solvent may lead to a phase separation of the melamine and PTCDI molecules, producing the "mixed" phase observed. It may be possible to characterize and reduce this effect and also to investigate whether it is due to nanoscale solvation in droplets, by increasing the desolvation of the ES beam; this is a design feature which will be included in future models of the ES apparatus. We estimate an upper limit for the kinetic energy of the impinging C_{60} molecules to be 360 meV, which is lower than the DFT calculated value for the PTCDI/melamine synthon binding energy, ~750 meV. This comparison of energies confirms that the supramolecular framework should be stable under the ES beam, but it does not preclude the possibility that clusters of molecules, or the impact of multiple molecules upon the same site, may be responsible for the change in network structure.

The results discussed above show that it is possible to deposit molecules onto a hydrogen-bonded supramolecular network, in UHV, using ES deposition without the need for additional "soft landing" measures.[32] The structures observed in the STM images provide clear evidence that C_{60} dimers and heptamers may be trapped within the network pores in a similar fashion to molecules which have been thermally sublimed. The similarities in the structures produced by the two deposition techniques show that the organization of the guest C_{60} molecules, that is, the size-selective trapping of molecules, is driven by similar microscopic processes, confirming UHV-ESD as a highly promising method for introducing guest moieties onto a prepre-pared (potentially fragile) nanostructured surface.

Conclusion

The viability of UHV-ESD for the deposition of molecules on a hydrogen-bonded network has been demonstrated. The nondestructive nature of the ES process, with respect to both deposited molecules and, partially, the hydrogen-bonded network, facilitates the investigation of the host–guest architecture for thermally labile, and/or nonvolatile, molecules which is not possible using conventional thermal techniques. Fragile molecules such as functionalized fullerenes, endohedral fullerenes, biomolecules, porphyrins, and single molecule magnets are all ideal candidates for future ES deposition experiments where optical, electronic, and structural information may be obtained for the adsorbed species.

Acknowledgment. This work was supported by the U.K. Engineering and Physical Sciences Research Council (EPSRC) under Grants GR/S97521/01 and EP/D048761/01, and the European Commission through the Early Stage Researcher Training Network MONET, MEST-CT-2005-020908.

References and Notes

(1) Harneit, W. *Phys. Rev. A* **2002**, *65*, 032322.
(2) Grill, L.; Dyeqr, M.; Lafferentz, L.; Parsson, M.; Peters, M. V.; Hecht, S. *Nat. Nanotechnol.* **2007**, *2*, 687–691.
(3) Rosei, F.; Schunack, M.; Naitoh, Y.; Jiang, P.; Gourdon, A.; Laegsgaard, I.; Stensgaard, I.; Joachim, C.; Besenbacher, F. *Prog. Surf. Sci.* **2003**, *71*, 95.
(4) Barth, J. V.; Costantini, G.; Kern, K. *Nature* **2005**, *437*, 671.
(5) Gatteschi, D.; Sessoli, R. *Angew. Chem., Int. Ed.* **2003**, *42*, 268–297.
(6) Fenn, J. B.; Mann, M.; Meng, C. K.; Wong, S. F.; Whitehouse, C. M. *Science* **1989**, *246*, 64–71.
(7) Rauschenbach, S.; Stadler, F. L.; Lunedei, E.; Malinowski, N.; Kolstov, S.; Costantini, G.; Kern, K. *Small* **2006**, *2*, 540–547.
(8) Lyon, J. E.; Cascio, A. J.; Beerbom, M. M.; Schalf, R.; Zhu, Y.; Jenekhe, S. A. *Appl. Phys. Lett.* **2006**, *88*, 222109.
(9) O'Shea, J. N.; Taylor, J. B.; Swarbrick, J.; Magnano, G.; Mayor, L. C.; Schulte, K. *Nanotechnology* **2007**, *18*, 035707–0357510.
(10) Satterley, C. J.; Perdigão, L. M. A.; Saywell, A.; Magnano, G.; Rienzo, A.; Mayor, L. C.; Dhanak, V. R.; Beton, P. H.; O'Shea, J. N. *Nanotechnology* **2007**, *18*, 455304.
(11) Barth, J. V.; Costantini, G.; Kern, K. *Nature* **2005**, *437*, 671–679.
(12) Theobald, J. A.; Oxtoby, N. S.; Phillips, M. A.; Champness, N. R.; Beton, P. H. *Nature* **2003**, *424*, 1029–10311.
(13) Stepanow, S.; Lin, N.; Vidal, F.; Landa, A.; Ruben, M.; Barth, J. V.; Kern, K. *Nano Lett.* **2005**, *5*, 901–904.
(14) Lu, J.; Lei, S.; Zeng, Q.; Kang, S.; Wang, C.; Wan, L.; Bai, C. *J. Phys. Chem. B* **2004**, *108*, 5161–5165.
(15) Griessl, S. J. H.; Lackinger, M.; Jamitzky, F.; Markert, T.; Hietschold, M.; Heckl, W. M. *Langmuir* **2004**, *20*, 9403–9407.
(16) Lackinger, M.; Griessl, S.; Heckl, W. A.; Hietschold, M.; Flynn, G. W. *Langmuir* **2005**, *21*, 4984–4988.
(17) Stepanow, S.; Lingenfelder, M.; Dmitriev, A.; Spillmann, H.; Delvigne, E.; Lin, N.; Deng, X.; Cai, C.; Barth, J. V.; Kern, K. *Nat. Mater.* **2004**, *3*, 229–233.
(18) Perdigão, L. M. A.; Perkins, E. W.; Ma, J.; Staniec, P. A.; Rogers, B. L.; Champness, N. R.; Beton, P. H. *J. Phys. Chem. B* **2006**, *110*, 12539–12542.
(19) Staniec, P. A.; Perdigão, L. M. A.; Saywell, A.; Champness, N. R.; Beton, P. H. *ChemPhysChem.* **2007**, *8*, 2177–2181.
(20) Stöhr, M.; Wahl, M.; Galka, C. H.; Riehm, T.; Jung, T. A.; Gade, L. H. *Angew. Chem., Int. Ed.* **2005**, *44*, 7394–7398.
(21) Zhanh, H. L.; Chen, W.; Chen, L.; Huang, H.; Wang, X. S.; Yuhura, J.; Wee, A. T. S. *Small* **2007**, *3*, 2015–2018.
(22) Spillmann, H.; Kiebele, A.; Stöhr, M.; Jung, T. A.; Bonifazi, O.; Cheng, F.; Diederich, F. *Adv. Mater.* **2006**, *18*, 275–279.
(23) Nath, K. G.; Ivasenko, O.; Miwa, J. A.; Dang, H.; Wuest, J. D.; Nanci, A.; Peripchka, D. F.; Rosei, F. *J. Am. Chem. Soc.* **2006**, *128*, 4212–4213.
(24) Xu, B.; Tao, C.; Cullen, W. G.; Reutt-Robey, J. E.; Williams, E. D. *Nano Lett.* **2005**, *5*, 2207–2211.
(25) Otero, R.; Schock, M.; Molina, L. M.; Laegsgaard, E.; Stensgaard, I.; Hammer, B.; Besenbacher, F. *Angew. Chem., Int. Ed.* **2005**, *44*, 2270–2275.
(26) Tahara, K.; Furukawa, S.; Uji-i, H.; Uchino, T.; Ichikawa, T.; Zhang, J.; Mamdouh, W.; Sonoda, M.; De Schryver, F. C.; De Feyter, S.; Tobe, Y. *J. Am. Chem. Soc.* **2006**, *128*, 16613–16625.
(27) Wu, D.; Keng, K.; Meng, H.; Zeng, Q.; Wang, C. *ChemPhysChem* **2007**, *8*, 1519.
(28) Images were processed using the WSxM Develop 10.0 free software from Nanotec Electronica S.L. (http://www.nanotec.es).
(29) Barth, J. V.; Brune, H.; Ertl, G.; Behm, R. J. *Phys. Rev. B* **1990**, *42*, 9307–9318.
(30) Swarbrick, J. C.; Ma, J.; Theobald, J. A.; Oxtoby, N. S.; O'Shea, J. N.; Champness, N. R.; Beton, P. H. *J. Phys. Chem. B* **2005**, *109*, 12167–12174.
(31) Calculations were performed using the DMol3 package.
(32) Hadjar, O.; Wang, P.; Futrell, J. H.; Dessiaterik, Y.; Zhu, Z.; Cowin, J. P.; Iedema, M. J.; Laskin, J. *Anal. Chem.* **2007**, *79*, 6566–6574.

JP7119944